Crowded chromatin is not sufficient for heterochromatin formation and not required for its maintenance

Andreas Walter[1‡], Catherine Chapuis[1,2,3] , Sébastien Huet[1,2,3*], and Jan Ellenberg[1*].

[1]Cell Biology and Biophysics Unit, European Molecular Biology Laboratory, D-69117 Heidelberg, Germany
[2]CNRS, UMR 6290, Institut Génétique et Développement de Rennes, F-35043 Rennes, France.
[3]Université de Rennes 1, Université Européenne de Bretagne, Structure fédérative de recherche Biosit , Faculté de Médecine, F-35043 Rennes, France

*Correspondence:

Sébastien Huet
Institut Génétique et du Développement de Rennes
Faculté de Médecine, 2 avenue du Professeur Léon Bernard
35043 Rennes Cedex, France
T +33 223234557
F +33 223234478
sebastien.huet@univ-rennes1.fr

Jan Ellenberg
European Molecular Biology Laboratory
Meyerhofstrasse 1
69117 Heidelberg, Germany
T +49 6221387328
F +49 62213878512
jan.ellenberg@embl.de

‡Present address: Max-Planck-Institut für Biophysik, Frankfurt am Main, Germany.

Running title : The role of crowding in heterochromatin biogenesis

Address to which proofs should be mailed :
Sébastien Huet
Institut Génétique et du Développement de Rennes
Faculté de Médecine, 2 avenue du Professeur Léon Bernard
35043 Rennes Cedex, France

ABSTRACT

In contrast to cytoplasmic organelles, which are usually separated from the rest of the cell by phospholipid membranes, nuclear compartments are readily accessible to diffusing proteins and must rely on different mechanisms to maintain their integrity. Specific interactions between scaffolding proteins are known to have important roles for the formation and maintenance of nuclear structures. General physical mechanisms such as molecular crowding, phase separation or colloidal behavior have also been suggested, but their physiological significance remains uncertain. For macromolecular crowding, a role in the maintenance of nucleoli and promyelocytic leukemia (PML) nuclear bodies has been shown. Here, we tested whether a modulation of the compaction state of chromatin, which directly influences the local crowding state, has an impact on the formation and maintenance of densely packed heterochromatin. By osmotic perturbations, we could modify the packing state of chromatin in a controlled manner and show that chromatin compaction, which is associated with increased crowding conditions, is not, *per se*, sufficient to initiate the formation of new *bona fide* heterochromatin structures nor is it necessary to maintain already established heterochromatin domains. In consequence, if an increase in crowding induced by chromatin compaction maybe an early step in heterochromatin formation, specific protein-protein interactions are nevertheless required to make heterochromatin long lasting and independent of the crowding state.

Keywords: Macromolecular crowding, chromatin, cell nucleus, fluorescence microscopy, osmotic perturbations, nuclear organelles

INTRODUCTION

During interphase, chromatin can be categorized into two different structural and functional states in the nucleus of eukaryotic cells. Heterochromatin remains highly compact during the entire interphase; it is characterized by a low density of genes and is mainly transcriptionally silent (Maison and Almouzni, 2004). In contrast, euchromatin corresponds to less compact and transcriptionally active chromatin. Several reports suggest that the high compaction levels observed in heterochromatin arise from a denser packing of the chromatin fiber (Dillon, 2004). The establishment of this specific chromatin architecture in heterochromatin is assumed to be mediated by post-transcriptional modifications of the histone tails which serve as binding sites for heterochromatin scaffolding proteins, which in turn favor additional histone modifications (Maison and Almouzni, 2004). The function of the high compaction of heterochromatin remains however unclear. The widespread assumption that this dense packing represses transcription by preventing access of RNA polymerase 2 has been challenged by the finding that heterochromatin is permeable to inert probes as large as RNA polymerase (Verschure et al., 2003; Bancaud et al., 2009). As an alternative function, we recently proposed that the dense fractal architecture of heterochromatin may regulate how rather than if transcriptional regulators bind chromatin (Bancaud et al., 2009). In addition to such potential functions in gene expression regulation, we and others have proposed that the macromolecular crowding resulting from the dense packing in heterochromatin plays a role in the biogenesis and maintenance of these nuclear domains (Rippe, 2007; Bancaud et al., 2009).

Heterochromatin, like many nuclear compartments, is stable for hours when observed microscopically, but at the same time highly dynamic at the molecular level (Snaar et al., 2000; Cheutin et al., 2003). To reconcile these two apparently contradictory characteristics, recent reports have proposed that such nuclear compartments are formed by self-organization mechanisms involving dynamic interactions between their constituent proteins (Dundr and Misteli, 2010). In addition, the self-organization processes could be strongly influenced by the local chromatin architecture (Rusche and Lynch, 2009; Keating, 2012). In heterochromatin, the high compaction makes these regions more crowded at the molecular level causing a significant fraction of the volume to be inaccessible for other molecules. In agreement with theoretical and *in-vitro* studies (Zhou et al., 2008; Cho and Kim, 2012), we could recently show that this *excluded volume effect* has two main consequences for the dynamics of macromolecules in heterochromatin: i) their diffusion is slowed down and ii) their binding reactions are shifted towards the bound state (Bancaud et al., 2009). These results led us to propose that enhanced macromolecular crowding could locally promote the binding of heterochromatin modifying and scaffolding proteins which in turn would cause more compaction. Such a positive feedback loop could be important to form or maintain heterochromatin foci. To be able to test this hypothesis, we now established an assay that allows predictable and reversible manipulation of the compaction state of chromatin in living cells. This allowed us to show that an enhancement of the molecular crowding associated with local chromatin compaction is not sufficient to create stable heterochromatin regions *de novo* that contain new scaffolding proteins. In addition, we found that the binding of heterochromatin scaffolding proteins is maintained even after decompaction of these domains, showing that a dense and crowded chromatin compaction state is not necessary for heterochromatin maintenance. Based on these findings we propose a model in which crowding induced by chromatin compaction may facilitate heterochromatin biogenesis

but where it requires specific protein-protein interactions to establish stable heterochromatin that then becomes independent of the crowding state.

MATERIAL AND METHODS

Fluorescent protein constructs

The plasmid constructs coding for the core histone H2B fused to enhanced GFP (EGFP), mCherry or the photoactivatable GFP (PA-GFP), as well as the one coding for the monomeric EGFP (mEGFP), were described previously (Snapp et al., 2003; Beaudouin et al., 2006; Mora-Bermúdez et al., 2007; Neumann et al., 2010). The coding sequence of pmCherry was used to generate the fluorescent tandem trimer mCherry-3. The HP1β and Suv39H1 genes were tagged with EGFP within a bacterial artificial chromosome (BAC).

Cell culture and osmotic shocks

NIH-3T3 cells were routinely cultured in Dulbecco's modified Eagle's medium (4.5 g/L glucose) supplemented with 10% fetal bovine serum, 2 mM glutamine, 100 µg/ml penicillin, 100 U/ml streptomycin and 1 mM sodium pyruvate in 5% CO_2 at 37°C. For the acquisitions on imaging setups, cells were plated on LabTekII-chambered coverglasses (Nunc, Roskilde, Denmark) and the growing medium was replaced by a CO_2-independent medium without phenol red (Invitrogen, Carlsbad, USA) supplemented with 20% fetal bovine serum, 2 mM glutamine, 100 µg/ml penicillin and 100 U/ml streptomycin. For the hypertonic shocks, this isotonic medium was replaced by imaging medium supplemented with 160 mM sucrose. For the hypotonic shocks, the imaging medium was diluted with distilled water until reaching a ratio of 35:65 v/v between imaging medium and water. The compositions of the hypertonic and hypotonic media were chosen to induce a rapid change of the chromatin compaction level without significantly precluding the cell viability after the osmotic shock. All the living cell experiments were performed at 37°C.

Cell transfection and stable cell lines

Transient transfections were performed using Fugene 6 (Roche, Basel, Switzerland), 24 h after plating. The cells were imaged 24-48 h after transfection. To establish NIH-3T3 cell lines expressing stably H2B-mCherry and HP1β-EGFP or Suv39H1-EGFP, wild-type cells were transfected with the cDNA or BAC constructs using Fugene 6 and Effectene (Qiagen, Hilden, Germany), respectively. Colonies of stable transformants were picked after two weeks of antibiotic selection.

Confocal imaging, fluorescence recovery after photobleaching or photoactivation

Confocal imaging and photoactivation experiments were performed on a Zeiss LSM 510 or a LSM 510 Meta (Carl Zeiss, Jena, Germany). Fluorescence recovery after photobleaching was performed on a TCS SP5 AOBS (acousto-optic beam splitter) confocal microscope (Leica Microsystems, Wetzlar, Germany). The cells were imaged using an oil immersion Plan-Apochromat 63x objective lens (N.A. 1.4). EGFP was excited with a 488-nm laser and mCherry

with a 543-nm or 561-nm laser. The PA-GFP was photoactivated with a 405-nm laser. The pinhole was set to one Airy unit for all channels. The dichroics and emission filters were chosen to optimize the collection of the emitted fluorescence in the different channels.

Immuno-fluorescence

NIH-3T3 cells expressing EGFP-H2B were fixed using 4%-paraformaldehyde and permeabilized with 0.2% Triton X-100 at room temperature or fixed with methanol at -20°C. Cells were stained using primary antibodies recognizing the trimethylation of histone H3 at lysine 9 (Abcam, Cambridge, USA), the trimethylation of histone H3 at lysine 4 (Merck Millipore, Darmstadt, Germany) or the serine 2 phosphorylation of the C-terminal domain of the RNA polymerase II (Abcam, Cambridge, USA). The secondary antibodies were labeled with Cyanine 3 (GE Healthcare, Chalfont St. Giles, UK) or Alexa Fluor 555 (Life Technologies, Carlsbad, USA).

DNA labeling with fluorescent nucleotides

NIH-3T3 cells were synchronized at the G1/S phase transition by a double 2mM thymidine block. The two blocks lasted 18h and 16h, separated by an incubation time of 8h in normal medium after the first release. After the second thymidine release, the cell layer, bathed with growing medium containing 10 µM of Cy3-dUTP (Jena-Bioscience, Jena, Germany), was scraped using a silicon stick to allow nucleotide loading (Schermelleh et al., 2001) and integration to the DNA during replication. To label specifically early, mid and late replicating DNA, the nucleotide labeling was performed immediately, 2h or 5h after thymidine release, respectively.

Fluorescence correlation spectroscopy

Fluorescence Correlation Spectroscopy (FCS) experiments were performed on a TCS SP2 AOBS confocal microscope (Leica Microsystems) using a water immersion Plan-Apochromat 63x objective lens (N.A. 1.2). The mEGFP was excited with a 488-nm laser. FCS raw data were acquired using an avalanche photodiode (Perkin-Elmer Optoelectronics, Fremont, USA) after a spectral filtering of the fluorescence light with a bandpass filter (BP500-550, Omega Optical, Brattleboro, USA). Each FCS acquisition was lasting at least 30 s to reduce the noise on the autocorrelation curves. When probing the diffusion of mEGFP in the nucleus of cells co-expressing mEGFP and H2B-mCherry, the accuracy in the position of the probed area could be verified *a-posteriori* by the local bleaching of the H2B-mCherry pattern visible at the site of the FCS acquisition. To estimate the residence time of mEGFP in the focal volume, the autocorrelation curves were fitted with a one-specie model assuming anomalous diffusion and neglecting the contribution of the photophysics of the mEGFP.

Automatic segmentation of the chromatin patterns

Confocal images of nuclei expressing EGFP-H2B or H2B-mCherry were smoothed using a moving average filter and segmented by Otsu thresholding to distinguish chromatin from the background and the nucleoli(Otsu, 1979). The distributions of pixel intensities in the chromatin

regions were fitted with a double Gaussian (fig. S1) and the intensity threshold between compacted and non-compacted chromatin was calculated as the mean of the central values for the two Gaussian. Due to the overlap between the two pixel intensity distributions, the compacted chromatin mask included small isolated structures within the non-compacted regions. These isolated structures were removed by applying an opening morphological filter with a circular kernel of radius 4 pixels to the compacted chromatin mask. The relative amount of compacted chromatin was thus obtained by dividing the number of pixels corresponding to compacted chromatin by the sum of all the chromatin pixels. For the cells bathed with isotonic medium, the non-compacted chromatin areas were identified as euchromatin and the compacted ones as heterochromatin. In nuclei subjected to hypertonic shocks, an additional opening filter with a circular kernel of radius 7 pixels was applied to the compacted chromatin areas to remove the fine network of compacted structures, attributed to newly compacted euchromatin, while preserving round heterochromatin area. Thus, three different segmentation masks were defined: (i) non-compacted euchromatin, (ii) heterochromatin and (iii) newly compacted euchromatin, this latter mask being obtained by subtracting the mask corresponding to compacted chromatin area with the heterochromatin mask.

Boxplots and statistical significance

On the displayed boxplots, the boxes have lines at the lower quartile, median, and upper quartile values. The whiskers extend from the boxes out to the most extreme data value within one interquartile range. The crosses represent the outliers, which are out of the range defined by the whiskers. To test for statistical significance, p-values were calculated using two-sided paired or unpaired t-tests. The unpaired t-tests were performed assuming unequal variances for the two samples.

RESULTS

Osmotic perturbations can acutely manipulate the compaction state of chromatin

In order to study the role of molecular crowding in the formation and maintenance of heterochromatin, we first established an assay allowing the manipulation of the compaction state of chromatin by subjecting cells to osmotic stress. We imaged by confocal microscopy NIH-3T3 mouse embryonic fibroblast cells expressing the core histone 2B (H2B) fused to EGFP and used the fluorescence intensities as a reporter of the local chromatin compaction level. By fitting the pixel intensity distributions derived from these images with a double Gaussian, we could automatically segment the bright regions and estimate the proportion of compacted chromatin within the nucleus (fig. S1). For cells bathed with isotonic medium, this assay allowed segmenting the prominent fluorescent spots corresponding to heterochromatin clustered in chromocenters (fig. 1A) but it probably does not have the resolution to distinguish between constitutive and facultative heterochromatin. We also observed that the relative amount of compacted chromatin remained stable during interphase, in agreement with the visual inspection of the image sequences.

Subjecting NIH-3T3 cells to hypertonic shocks by incubating them with isotonic medium supplemented with 160 mM sucrose led to chromatin hyper-compaction evidenced by the

appearance of multiple bright dense structures on the EGFP-H2B patterns (fig. 1B). The segmentation and quantification of these images showed that hypertonic shocks induced a rapid increase of the relative amount of compacted chromatin in the treated nuclei. The chromatin compaction upon hypertonic shock was associated with a decrease of the nuclear volume by nearly 30 % (fig. S2A). Following the initial hyper-compaction, chromatin slowly decompacted as cells adapted to the hypertonic medium within approximately one hour. Similar results were obtained when incubating cells with isotonic medium supplemented with 120 mM NaCl (data not shown).

Furthermore, we investigated whether some chromatin regions could be more prone to compaction upon hypertonic shock than others. Early, mid and late replicating DNA were labeled with fluorescent nucleotides and the relative chromatin compaction level, assessed by the Hoechst signal, was measured at the nucleotide integration sites in cells bathed with isotonic or hypertonic medium (Fig S2B). The dense heterochromatic chromocenters were excluded from this analysis. Our results suggest that the early replicating DNA shows a greater tendency to compact upon hypertonic shock than the mid or late replicating DNA.

Incubating cells with hypotonic medium (isotonic medium diluted with water, 35:65 v/v) led to a rapid smoothing of the EGFP-H2B patterns visible on the images of the fluorescent nuclei (fig. 1C). This was due to decompaction of chromatin and not release of H2B from DNA as tested by photoactivation of H2B tagged with photoactivatable GFP, which remained immobilized in hypotonic conditions (fig. S2C). Heterochromatin foci were almost completely decompacted under hypotonic conditions, indistinguishable in compaction from the rest of the chromatin. This was confirmed by the automatic estimation of the relative amount of compacted chromatin, which showed a dramatic and rapid drop upon addition of the hypotonic medium (fig. 1C). This chromatin decompaction was associated with an increase of the nuclear volume by about 40 % (fig. S2A). Following the rapid decompaction of the chromatin, cells progressively adapted to the hypotonic medium over several hours following the shock, and reestablished a significant amount of compacted chromatin.

Modifying chromatin compaction level changes the crowding state

To test how the modulation of chromatin compaction levels by osmotic stress affects the local crowding state of the nucleus, we measured the exclusion and diffusion slow down of inert tracers in compact or non-compact chromatin identified by fluorescently labeled H2B. In isotonic conditions, a tandem trimer of mCherry (mCherry-3) was evenly distributed in euchromatin and largely excluded from heterochromatin (Fig. 2A, upper row). Upon hypertonic shocks, we observed a partial exclusion of mCherry-3 from the newly compacted euchromatin regions (fig. 2A, blue arrowheads). Automatic segmentation of the H2B patterns (see methods) allowed us to quantitatively compare the exclusion of the diffusive tracer mCherry-3 from euchromatin newly compacted by hypertonic treatment with exclusion from heterochromatin in isotonic conditions (fig. 2B). mCherry-3 was excluded from newly compacted euchromatin to a similar extent as from heterochromatin in isotonic conditions (fig. 2B), demonstrating that nuclear areas with dense chromatin induced by hypertonic conditions are indeed more crowded. Next, the diffusion of mEGFP was quantified in nuclear areas with different degrees of chromatin compaction using fluorescence correlation spectroscopy (FCS). In isotonic conditions

and in agreement with our previous findings (Bancaud et al., 2009), a slowing down of the diffusion of mEGFP by a factor of ~2 was measured in heterochromatin as compared to euchromatin (fig. 2C). In nuclei subjected to hypertonic shocks, the mobility of mEGFP within the newly compacted chromatin regions was similar to heterochromatin in isotonic conditions (fig. 2C). Thus the crowding conditions encountered in the hypertonically compacted euchromatin are similar to those of isotonic heterochromatin.

To test if crowding is indeed reduced in heterochromatin foci decompacted by hypotonic conditions, we quantified the exclusion of mCherry-3 in these regions before and after the perturbation in cells co-expressing mCherry-3 and EGFP-H2B. To allow identifying the position of heterochromatin foci after the shock, the nuclei were also labeled with Hoechst. Indeed, while the EGFP-H2B spots disappeared upon chromatin decompaction induced by hypotonic shocks, the heterochromatin foci were still visible on the Hoechst channel due to the preferential binding of this dye to the AT-enriched heterochromatin DNA regions (Petit et al., 1993). Using this assay, we found that the decompaction of heterochromatin by hypotonic shock led to loss of the volume exclusion of mCherry-3 within these regions (fig. 3), suggesting that hypotonically decompacted heterochromatin has a similarly low level of molecular crowding as euchromatin.

Newly compacted euchromatin lacks heterochromatin marks

Constitutive heterochromatin is characterized by specific post-transcriptional histone modifications, including histone 3 lysine 9 tri-methylation (H3K9me3) (Maison and Almouzni, 2004). Two proteins play a key role in the dynamic maintenance of this histone mark: the methyltransferase Suv39H1, which methylates the H3K9 and the chromatin-binding protein HP1, which recognizes the methylated H3K9 and is presumed to function in stabilizing and spreading the heterochromatic region (Maison and Almouzni, 2004). Both HP1 and Suv39H1 bind dynamically to chromatin all over the nucleus, but with a higher affinity for heterochromatin (Cheutin et al., 2003; Krouwels et al., 2005). Having shown that hypertonically compacted euchromatin is indistinguishable in molecular crowding from heterochromatin, we now wanted to test whether this local increase of crowding would be sufficient to promote the accumulation of HP1 and Suv39H1, and thus lead to the formation of new stable heterochromatin regions.

NIH-3T3 cells co-expressing H2B-mCherry and the isoform β of HP1 (HP1β) or Suv39H1 fused to EGFP were subjected to hypertonic conditions and assayed at least five minutes after the perturbation by confocal microscopy. Despite the marked compaction of euchromatin as visualized in the H2B channel, the distribution of HP1β was only slightly affected by the hypertonic shock (fig. 4A) and only a moderate clustering of Suv39H1 could be observed within the newly compacted euchromatin areas. To test if HP1β or Suv39H1 bound to the newly compacted euchromatin are above the levels expected from their low level binding to uncompacted euchromatin, we measured the fluorescence intensity increase of HP1β and Suv39H1 after the hypertonic perturbation relative to H2B (fig. 4B) in regions of interest containing newly compacted euchromatin (fig. S3A). As a control we used cells co-expressing H2B-mCherry and EGFP-H2B, which showed the same increase in both channels. The fluorescence gains for both HP1β and Suv39H1 were significantly lower than for H2B, suggesting that the binding of these proteins to compacted euchromatin was partially impaired

(fig. 4B). Thus, none of the two scaffolding heterochromatin proteins that we tested showed an enhanced binding in newly compacted euchromatin.

To exclude that the hypertonic perturbation immobilized HP1β and Suv39H1 and thereby prevented their relocation and binding to newly compacted chromatin regions, we measured the dynamics of both proteins by Fluorescence Recovery After Photobleaching (FRAP) (fig. S4). Although the kinetics of HP1 recovery was slowed down, both HP1β and Suv39H1 almost completely re-equilibrated over the entire nucleus within a few minutes after FRAP in hypertonic conditions, which excludes that they are not available for binding to newly compacted chromatin.

To investigate if the activity of Suv39H1 was enhanced by the local compaction of euchromatin, we tested if hypertonic perturbations led to an increase of H3K9 methylation. Cells expressing EGFP-H2B were subjected to hypertonic perturbation, fixed after 15 and 45 min and stained against H3K9 tri-methylation (H3K9me3). While the strong methylation signal in heterochromatin foci was not affected, we could see no obvious increase of H3K9me3 in newly compacted euchromatin induced by the hypertonic perturbation (fig. 4C). Thus neither localization nor activity of Suv39H1 appeared to be enhanced in newly compacted euchromatin.

In order to further characterize the transcriptional state of euchromatin compacted by hypertonic shocks, the localizations of additional histone marks were analyzed. Up to 45 min after the shocks, no specific accumulation of H3K27 tri-methylation, which is associated with facultative heterochromatin (Trojer and Reinberg, 2007), could be detected in these regions (fig. S5). In addition, the H3K4 tri-methylation, a classical mark for active chromatin (Schübeler et al., 2004), and the elongating RNA polymerase II (phosphorylated on the serine 2 of the C-terminal domain (Heidemann et al., 2013)) were both partially excluded from newly compacted euchromatin (fig. S5). This exclusion was already visible 5 min after the hypertonic shock and remained stable during the 45 min following the shock.

Heterochromatin scaffolding proteins and histone marks are stable after decompaction

Even though increased molecular crowding was not sufficient for the formation of new *bona fide* heterochromatin foci, it could be necessary for the maintenance of already established heterochromatin regions. To test this hypothesis, we first analyzed the impact of chromatin decompaction on the binding of Suv39H1 and HP1β in heterochromatin. When cells expressing Suv39H1-EGFP or HP1β-EGFP together with H2B-mCherry were subjected to hypotonic perturbations, both HP1β and Suv39H1 remained accumulated in heterochromatin even after complete decompaction of the foci (fig. 5A). To quantify if Suv39H1 or HP1β were lost from heterochromatin upon chromatin decompaction, we measured the fluorescence intensity of HP1β and Suv39H1 after the hypotonic perturbation relative to H2B in regions encompassing the heterochromatin foci before and after the perturbation based on segmentation of HP1β and Suv39H1 (fig. S3B). While the total intensity of H2B was expected to be conserved after heterochromatin decompaction, the fluorescence intensity of Suv39H1 or HP1β proteins should decrease after hypotonic perturbation if maintenance of their binding relies on high molecular crowding in heterochromatin. As a control we again used cells co-expressing H2B-mCherry and

EGFP-H2B in which heterochromatin decompaction was incomplete to allow its segmentation based on the core histone signal only. As expected, there was no significant change in both channels (fig. 5B). For HP1β, the intensity within heterochromatin did not change significantly upon hypotonic shock while for Suv39H1 we even observed an increase of the intensity within the decompacted heterochromatin. Thus, maintaining the binding of HP1β and Suv39H1 to heterochromatin does not require compact heterochromatin.

To exclude that the hypotonic perturbation immobilized HP1β and Suv39H1 in heterochromatin and thereby prevented their unbinding after decompaction, we measured the dynamics of both proteins by FRAP (fig. S4). While the dynamics of Suv39H1 remained unchanged compared to isotonic conditions, the redistribution of HP1β was even accelerated after hypotonic treatment. Thus, both proteins remained mobile after the hypotonic perturbation and kept shuttling between euchromatin and heterochromatin within timescales of a few minutes, which excludes that they are unable to dissociate from heterochromatin.

Finally, we also analyzed whether the high chromatin compaction state of heterochromatin was required for the maintenance of the H3K9 tri-methylation. Cells expressing EGFP-H2B were subjected to hypotonic perturbation and fixed and stained against H3K9me3 after 15, 45 or 180 min respectively. The strong methylation signal of heterochromatin foci was unaffected for up to three hours after the hypotonic perturbation (fig. 5C), indicating that chromatin decompaction did not affect the maintenance of this classical heterochromatin histone mark.

DISCUSSION

Reversible manipulation of the chromatin compaction state by osmotic stress

In agreement with previous reports (Brasch et al., 1971; Richter et al., 2007), we observed that hyper- or hypotonic perturbations led to a dramatic, but reversible, chromatin hyper- or decompaction, respectively (fig. 1). Previous studies have suggested that both the cation concentration (Martin and Cardoso, 2010) and the intracellular crowding (Cunha et al., 2001; Iborra, 2007; Richter et al., 2007) can affect the chromatin compaction state. The abrupt changes of the nuclear volume observed upon osmotic stress (fig S2.) are likely to have a strong impact on the nuclear crowding level, which could in turn cause chromatin hyper- or decompaction. However, the nuclear double membrane is pierced with nuclear pores that only restrict diffusional equilibration above ~40 kDa (Keminer and Peters, 1999). Since this membrane does not insulate the nucleus entirely from the cytoplasm concerning the solute concentration, the changes in intracellular ion concentrations associated with the osmotic shocks could also contribute to the modification of the chromatin compaction state (Delpire et al., 1985; Martin and Cardoso, 2010). In this context, our observation that the early replicating chromatin is more prone to compaction upon hypertonic treatment than mid or late replicating regions (fig. S2) suggest that the sensitivity of the chromatin structure to the local crowding and ionic conditions may be different from one chromatin region to the other. Importantly, osmotic shocks modify chromatin compaction acutely within seconds and act independent of histone marks such as the heterochromatin specific H3K9 tri-methylation. This is in contrast to alternative

pharmacological approaches inhibiting histone deacetylases (e.g. sodium butyrate, trichostatin A), that lead to chromatin decompaction, but require several hours of incubation and change histone marks (Görisch et al., 2005).

Modifying the chromatin compaction state by osmotic stress influences the local level of crowding in the nucleus

By characterizing the exclusion and diffusion slow-down of fluorescent tracers within nuclei subjected to osmotic stress, we could show that the local crowding is strongly influenced by the chromatin compaction level. Indeed, the euchromatin areas that got compacted upon hypertonic shocks were characterized by enhanced crowding conditions as compared to the surrounding euchromatin (fig. 2), thus mimicking the differences observed between heterochromatin and euchromatin in isotonic medium. We also found that the strong crowding conditions characterizing isotonic heterochromatin could be abolished by decompacting these regions with hypotonic shocks (fig. 3). Together with previous reports (Martin and Cardoso, 2010), these results suggest that chromatin, which is thought to occupy ~50 % of the nuclear volume (Rouquette et al., 2009), is the main crowding agent within the nucleus. Thus, modifying the level of chromatin compaction has a direct impact on the local crowding in the nucleus. Our observations also show that, because of this ability to locally affect the nuclear crowding, osmotic perturbations could be a useful tool to understand the role of molecular crowding in nuclear processes.

Chromatin hyper-compaction associated with local enhancement of molecular crowding is not sufficient for the *de novo* formation of stable heterochromatin

De novo formation of nuclear compartments occurs in response to external triggers (Lavau et al., 1995; Sleeman et al., 2001) and after cell division concomitant with nuclear assembly (Dundr and Misteli, 2010). It is generally assumed that the establishment of new nuclear compartments involves self-organization processes (Rajendra et al., 2010). Following an initial nucleation event, whose exact nature remains elusive, the subsequent binding of diffusing scaffolding proteins and dynamic binding partners is thought to induce the expansion of the compartment till it reaches a steady-state size. In addition to the molecular players participating in these assembly steps, molecular crowding facilitates the formation of different nuclear compartments (Hancock, 2004; Iborra, 2007; Rippe, 2007). It is however unclear if crowding is involved at the nucleation step and/or during the growing phase. In this report, we show that the local compaction of chromatin, which is associated with an enhancement of the molecular crowding, does not, *per se*, constitute a nucleation event initiating the formation of new heterochromatin foci, as no accumulation of HP1β, Suv39H1 or heterochromatin-specific histone marks could be observed in hypertonically compacted euchromatin (fig. 3). Moreover cells returned to a normal eu- and heterochromatin balance within an hour after hypertonic perturbation (fig. 1). Cells can experience modifications of their osmotic environment in response to different events. For example, articular cartilage tissues react to mechanical forces by exuding water, leading to an increase of osmotic pressure experienced by the cells of these tissues (Finan and Guilak, 2010). The resistance to initiate heterochromatin from hypertonically compacted euchromatin regions could be important to avoid the spontaneous silencing of genes if cells encounter a change in their environment. Nevertheless, we also observed an exclusion of

several marks of actively transcribing chromatin from the newly compacted regions (fig. S5). Thus, it is possible that a more prolonged hypertonically induced compaction would be required to start *de novo* heterochromatinization, which was not possible to achieve experimentally due to the adaptation of cells to hypertonic conditions within one hour. In addition, our data does not exclude that the increased molecular crowding induced by chromatin compaction could play a facilitating role during the growth phase of heterochromatin, by locally promoting the binding of additional heterochromatin scaffolding proteins.

A dense and crowded chromatin packing is not required for the maintenance of heterochromatin

The specific architecture of the chromatin fiber in heterochromatin allows a very tight packing of the genetic material in these areas (Dillon, 2004). If this compact structure also has functional consequences remains an actively debated question. Our results, that HP1β, Suv39H1 and heterochromatin-specific histone marks remained accumulated within heterochromatin despite the decompaction of the foci for up to three hours after hypotonic perturbation, suggest that dense heterochromatin packing and high molecular crowding, are not required to maintain the molecular identity of heterochromatin foci. This is further supported by the fact that chromatin re-compacts in very similar patterns, during the recovery phase following the hypotonic shocks (fig. 1C), exhibiting a "structural memory". In the case of constitutive heterochromatin, this memory may involve stable platforms composed of proteins that bind very tightly to chromatin such as Suv420H or Ki-67 (Hemmerich et al., 2011).

Nuclear compartments can be separated into two broad categories, those associated with specific chromatin regions, such as nucleoli and heterochromatin foci, or those that do not contain chromatin, including for example PML bodies or paraspeckles. While the first category can use chromatin as a structural platform for their dynamic steady state maintenance, the second type of compartments can only rely on the transient interactions between diffusing scaffolding proteins to preserve their integrity. Molecular crowding has been shown to be involved in the maintenance of organelles from both groups, nucleoli and PML bodies (Hancock, 2004). Here, our data suggest that heterochromatin foci, which similar to nucleoli are associated with specific chromatin domains, do not require a dense and crowded chromatin packing for their maintenance, suggesting that the physical mechanisms underlying the dynamic maintenance of nuclear compartments may be different from one compartment to the other.

ACKNOWLEDGMENTS

We thank Marc Tramier and Wanqing Xiang for critical reading of the manuscript. We are grateful to the members of the Advanced Light Microscopy Facility at the European Molecular Biology Laboratory, and of the Microscopy Rennes Imaging Center for technical assistance with the microscopes. S.H. was supported by a fellowship from the European Molecular Biology Organization. S.H. and C.C. were supported by grants from the Agence National de la Recherche (JCJC-SVSE2-2011, ChromaTranscript project) and from the European Union (FP7-PEOPLE-2011-CIG, ChromaTranscript project)

REFERENCES

Bancaud, A., Huet, S., Daigle, N., Mozziconacci, J., Beaudouin, J., Ellenberg, J., 2009. Molecular crowding affects diffusion and binding of nuclear proteins in heterochromatin and reveals the fractal organization of chromatin. EMBO J 28, 3785–3798.

Beaudouin, J., Mora-Bermúdez, F., Klee, T., Daigle, N., Ellenberg, J., 2006. Dissecting the contribution of diffusion and interactions to the mobility of nuclear proteins. Biophys. J 90, 1878–1894.

Brasch, K., Seligy, V.L., Setterfield, G., 1971. Effects of low salt concentration on structural organization and template activity of chromatin in chicken erythrocyte nuclei. Exp. Cell Res 65, 61–72.

Cheutin, T., McNairn, A.J., Jenuwein, T., Gilbert, D.M., Singh, P.B., Misteli, T., 2003. Maintenance of stable heterochromatin domains by dynamic HP1 binding. Science 299, 721–725.

Cho, E.J., Kim, J.S., 2012. Crowding effects on the formation and maintenance of nuclear bodies: insights from molecular-dynamics simulations of simple spherical model particles. Biophys. J. 103, 424–433.

Cunha, S., Woldringh, C.L., Odijk, T., 2001. Polymer-mediated compaction and internal dynamics of isolated Escherichia coli nucleoids. J. Struct. Biol. 136, 53–66.

Delpire, E., Duchêne, C., Goessens, G., Gilles, R., 1985. Effects of osmotic shocks on the ultrastructure of different tissues and cell types. Exp. Cell Res. 160, 106–116.

Dillon, N., 2004. Heterochromatin structure and function. Biol. Cell 96, 631–637.

Dundr, M., Misteli, T., 2010. Biogenesis of nuclear bodies. Cold Spring Harb Perspect Biol 2, a000711.

Finan, J.D., Guilak, F., 2010. The effects of osmotic stress on the structure and function of the cell nucleus. J. Cell. Biochem. 109, 460–467.

Görisch, S.M., Wachsmuth, M., Tóth, K.F., Lichter, P., Rippe, K., 2005. Histone acetylation increases chromatin accessibility. J. Cell. Sci. 118, 5825–5834.

Hancock, R., 2004. A role for macromolecular crowding effects in the assembly and function of compartments in the nucleus. J. Struct. Biol. 146, 281–290.

Heidemann, M., Hintermair, C., Voß, K., Eick, D., 2013. Dynamic phosphorylation patterns of RNA polymerase II CTD during transcription. Biochim. Biophys. Acta 1829, 55–62.

Hemmerich, P., Schmiedeberg, L., Diekmann, S., 2011. Dynamic as well as stable protein interactions contribute to genome function and maintenance. Chromosome Res. 19, 131–151.

Iborra, F.J., 2007. Can visco-elastic phase separation, macromolecular crowding and colloidal physics explain nuclear organisation? Theor Biol Med Model 4, 15.

Keating, C.D., 2012. Aqueous phase separation as a possible route to compartmentalization of biological molecules. Acc. Chem. Res. 45, 2114–2124.

Keminer, O., Peters, R., 1999. Permeability of single nuclear pores. Biophys. J. 77, 217–228.

Krouwels, I.M., Wiesmeijer, K., Abraham, T.E., Molenaar, C., Verwoerd, N.P., Tanke, H.J., Dirks, R.W., 2005. A glue for heterochromatin maintenance: stable SUV39H1 binding to heterochromatin is reinforced by the SET domain. J. Cell Biol. 170, 537–549.

Lavau, C., Marchio, A., Fagioli, M., Jansen, J., Falini, B., Lebon, P., Grosveld, F., Pandolfi, P.P., Pelicci, P.G., Dejean, A., 1995. The acute promyelocytic leukaemia-associated PML gene is induced by interferon. Oncogene 11, 871–876.

Maison, C., Almouzni, G., 2004. HP1 and the dynamics of heterochromatin maintenance. Nat. Rev. Mol. Cell Biol. 5, 296–304.
Martin, R.M., Cardoso, M.C., 2010. Chromatin condensation modulates access and binding of nuclear proteins. FASEB J. 24, 1066–1072.
Mora-Bermúdez, F., Gerlich, D., Ellenberg, J., 2007. Maximal chromosome compaction occurs by axial shortening in anaphase and depends on Aurora kinase. Nat. Cell Biol 9, 822–831.
Neumann, B., Walter, T., Hériché, J.-K., Bulkescher, J., Erfle, H., Conrad, C., Rogers, P., Poser, I., Held, M., Liebel, U., Cetin, C., Sieckmann, F., Pau, G., Kabbe, R., Wünsche, A., Satagopam, V., Schmitz, M.H.A., Chapuis, C., Gerlich, D.W., Schneider, R., Eils, R., Huber, W., Peters, J.-M., Hyman, A.A., Durbin, R., Pepperkok, R., Ellenberg, J., 2010. Phenotypic profiling of the human genome by time-lapse microscopy reveals cell division genes. Nature 464, 721–727.
Otsu, N., 1979. Threshold selection method from gray-level histograms. IEEE Trans. Syst. Man Cybern. 9, 62–66.
Petit, J.M., Denis-Gay, M., Ratinaud, M.H., 1993. Assessment of fluorochromes for cellular structure and function studies by flow cytometry. Biol. Cell 78, 1–13.
Rajendra, T.K., Praveen, K., Matera, A.G., 2010. Genetic analysis of nuclear bodies: from nondeterministic chaos to deterministic order. Cold Spring Harb. Symp. Quant. Biol. 75, 365–374.
Richter, K., Nessling, M., Lichter, P., 2007. Experimental evidence for the influence of molecular crowding on nuclear architecture. J. Cell. Sci. 120, 1673–1680.
Rippe, K., 2007. Dynamic organization of the cell nucleus. Curr. Opin. Genet. Dev. 17, 373–380.
Rouquette, J., Genoud, C., Vazquez-Nin, G.H., Kraus, B., Cremer, T., Fakan, S., 2009. Revealing the high-resolution three-dimensional network of chromatin and interchromatin space: a novel electron-microscopic approach to reconstructing nuclear architecture. Chromosome Res. 17, 801–810.
Rusche, L.N., Lynch, P.J., 2009. Assembling heterochromatin in the appropriate places: A boost is needed. J. Cell. Physiol. 219, 525–528.
Schermelleh, L., Solovei, I., Zink, D., Cremer, T., 2001. Two-color fluorescence labeling of early and mid-to-late replicating chromatin in living cells. Chromosome Res 9, 77–80.
Schübeler, D., MacAlpine, D.M., Scalzo, D., Wirbelauer, C., Kooperberg, C., van Leeuwen, F., Gottschling, D.E., O'Neill, L.P., Turner, B.M., Delrow, J., Bell, S.P., Groudine, M., 2004. The histone modification pattern of active genes revealed through genome-wide chromatin analysis of a higher eukaryote. Genes Dev. 18, 1263–1271.
Sleeman, J.E., Ajuh, P., Lamond, A.I., 2001. snRNP protein expression enhances the formation of Cajal bodies containing p80-coilin and SMN. J. Cell. Sci. 114, 4407–4419.
Snaar, S., Wiesmeijer, K., Jochemsen, A.G., Tanke, H.J., Dirks, R.W., 2000. Mutational analysis of fibrillarin and its mobility in living human cells. J. Cell Biol. 151, 653–662.
Snapp, E.L., Hegde, R.S., Francolini, M., Lombardo, F., Colombo, S., Pedrazzini, E., Borgese, N., Lippincott-Schwartz, J., 2003. Formation of stacked ER cisternae by low affinity protein interactions. J. Cell Biol. 163, 257–269.
Trojer, P., Reinberg, D., 2007. Facultative heterochromatin: is there a distinctive molecular signature? Mol. Cell 28, 1–13.
Verschure, P.J., van der Kraan, I., Manders, E.M.M., Hoogstraten, D., Houtsmuller, A.B., van Driel, R., 2003. Condensed chromatin domains in the mammalian nucleus are accessible to large macromolecules. EMBO Rep 4, 861–866.

Zhou, H.-X., Rivas, G., Minton, A.P., 2008. Macromolecular crowding and confinement: biochemical, biophysical, and potential physiological consequences. Annu Rev Biophys 37, 375–397.

FIGURE LEGENDS

Figure 1: Effect of osmotic stress on the chromatin compaction state in living cells. Living 3T3 cells expressing EGFP-H2B were imaged by confocal microscopy for several hours to study the consequences of osmotic stress on the chromatin compaction state. The chromatin pattern was imaged for cells bathed in isotonic (A), hypertonic (B) and hypotonic (C) media. Bar = 4 μm. Time is indicated in h:min. The raw images of the EGFP-H2B patterns were segmented automatically to distinguish compacted chromatin regions from the rest of the chromatin. The result of the segmentation is shown below the raw image sequences with green regions corresponding to compacted chromatin areas. The graphs on the right display the variations of the amount of compacted chromatin relative to the first time point, that were derived from the segmentation procedure. The purple dots correspond to the proportions of compacted chromatin calculated for the images shown on the left. The green curves were obtained by interpolating the data points after having smoothed them using a median filter. The black arrows indicate the time of the osmotic shock.

Figure 2: Crowding conditions in hypertonically compacted euchromatin are similar to those encountered in isotonic heterochromatin. (A) Living 3T3 cells co-expressing EGFP-H2B and mCherry-3 were imaged by confocal microscopy to visualize the exclusion of mCherry-3 from dense chromatin areas. The EGFP-H2B and mCherry-3 patterns were imaged before and after hypertonic shocks. Bar = 4 μm. The fluorescence intensity profiles shown on the right for EGFP-H2B and mCherry-3 were measured along the green or red dotted lines, respectively, and normalized against the mean intensity along the profile. The orange arrowhead corresponds to a heterochromatin focus and the blue arrowheads indicate two hypertonically compacted euchromatin regions. (B) The image on the left is the result of the segmentation for the raw images displayed in (A). Based on this segmentation, the concentrations of mCherry-3 in heterochromatin and compacted euchromatin, were estimated relative to non-compacted euchromatin. The boxplot shows the result of this quantification performed on 13 cells imaged successively in isotonic and hypertonic conditions. The green and blue boxes correspond to the relative concentrations of mCherry-3 in isotonic heterochromatin and hypertonically compacted euchromatin, respectively. Unpaired t-tests were used to test for statistical significance. (C) The diffusion of mEGFP was characterized by FCS at different locations in the nucleus of cells co-expressing H2B-mCherry and mEGFP. Shown on the left are the normalized autocorrelation curves at different nuclear locations for a typical cell. The raw data (dots) were fitted (plain and dotted lines) to estimate the characteristic residence times of mEGFP in the focal volume. The boxplot displays the residence times estimated for 10 cells before and after hypertonic shocks. The red, green and blue boxes correspond to the residence times measured in isotonic euchromatin, heterochromatin and in hypertonically compacted euchromatin. Shown p-values were calculated by unpaired t-tests.

Figure 3: Enhanced crowding in heterochromatin is lost upon decompaction of the heterochromatin foci by hypotonic shocks. (A) Living 3T3 cells co-expressing EGFP-H2B and mCherry-3 and labeled with Hoechst were imaged successively by confocal microscopy before and after hypotonic shocks to visualize the exclusion of mCherry-3 from heterochromatin. Insets are pseudocolored, 1.5-fold magnified views of the heterochromatin focus indicated by the red square. Bar = 4 μm. (B) Shown are the concentration ratios for mCherry-3 between heterochromatin and euchromatin measured in 8 cells imaged successively before and after hypotonic shocks. For each cell, the mCherry-3 concentrations were measured within three manually chosen euchromatic and heterochromatic areas, delineated based on the Hoechst patterns. Statistical significance was estimated by a paired t-test.

Figure 4: The local compaction of euchromatin by hypertonic shocks is not sufficient to initiate the formation of new heterochromatin areas.
(A) Confocal images of living 3T3 cells expressing HP1β-EGFP or Suv39H1-EGFP together with H2B-mCherry and bathed with isotonic or hypertonic media. Insets are pseudocolored, 1.5-fold magnified views of the euchromatin areas indicated by the red squares. Bar = 4 μm. (B) Shown are the relative variations upon hypertonic shocks of the integrated fluorescence intensities for H2B, HP1β and Suv39H1 within hypertonically compacted euchromatin (12 cells co-expressing HP1β-EGFP and H2B-mCherry and 11 cells co-expressing Suv39H1-EGFP and H2B-mCherry, 3 ROIs per nucleus). The regions where we measured the fluorescence intensities were defined manually based on the H2B patterns after the shocks. The fluorescence intensities in the hypertonic conditions were measured at least 5 minutes after the shock. As a control, the intensity variations upon hypertonic shocks of EGFP-H2B and H2B-mCherry within hypertonically compacted euchromatin were estimated in 8 nuclei co-expressing the two constructs. p-values were calculated by paired t-tests. (C) Confocal images of 3T3 cells expressing EGFP-H2B, fixed at different times after hypertonic shocks, as indicated above the images, and stained with an antibody against the histone 3 trimethylated at lysine 9 (H3K9me3). Insets are pseudocolored, 1.5-fold magnified views of the regions indicated by the red squares. Bar = 4 μm.

Figure 5: Dense chromatin packing is not necessary for the maintenance of heterochromatin. (A) Confocal images of living 3T3 cells expressing HP1β-EGFP or Suv39H1-EGFP together with H2B-mCherry and bathed with isotonic or hypotonic media. Insets are pseudocolored, 1.5-fold magnified views of the heterochromatin foci indicated by the red squares. Bar = 4 μm. (B) Shown are the relative variations upon hypotonic shocks of the integrated fluorescence intensities for H2B, HP1β and Suv39H1 within heterochromatin (13 cells for both HP1β-EGFP / H2B-mCherry and Suv39H1-EGFP / H2B-mCherry co-expressions). For each nucleus, three heterochromatin foci were delineated manually before and after the shocks on the images in the HP1β or Suv39H1 channels. The fluorescence intensities in the hypotonic conditions were measured at least 5 minutes after the shocks. As a control, the intensity variations upon hypotonic shocks of EGFP-H2B and H2B-mCherry within heterochromatin foci were estimated in 8 nuclei co-expressing the two constructs. Displayed p-values were calculated by paired t-tests. (C) Confocal images of 3T3 cells expressing EGFP-H2B, fixed at different times after hypotonic shocks, as indicated above the images, and stained with an antibody against the histone 3 trimethylated at lysine 9 (H3K9me3). Bar = 4 μm.

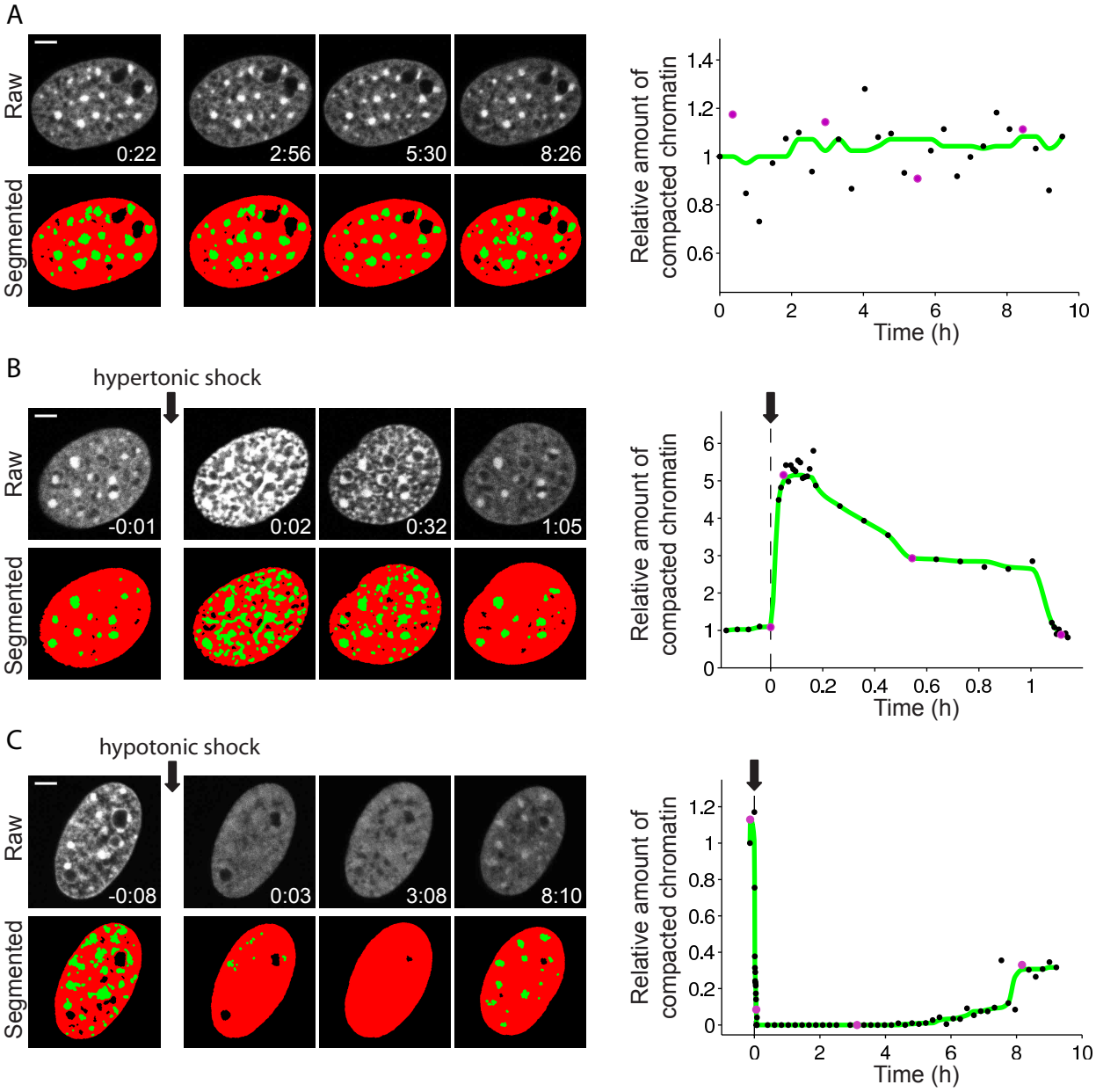

Walter et al., Figure 1

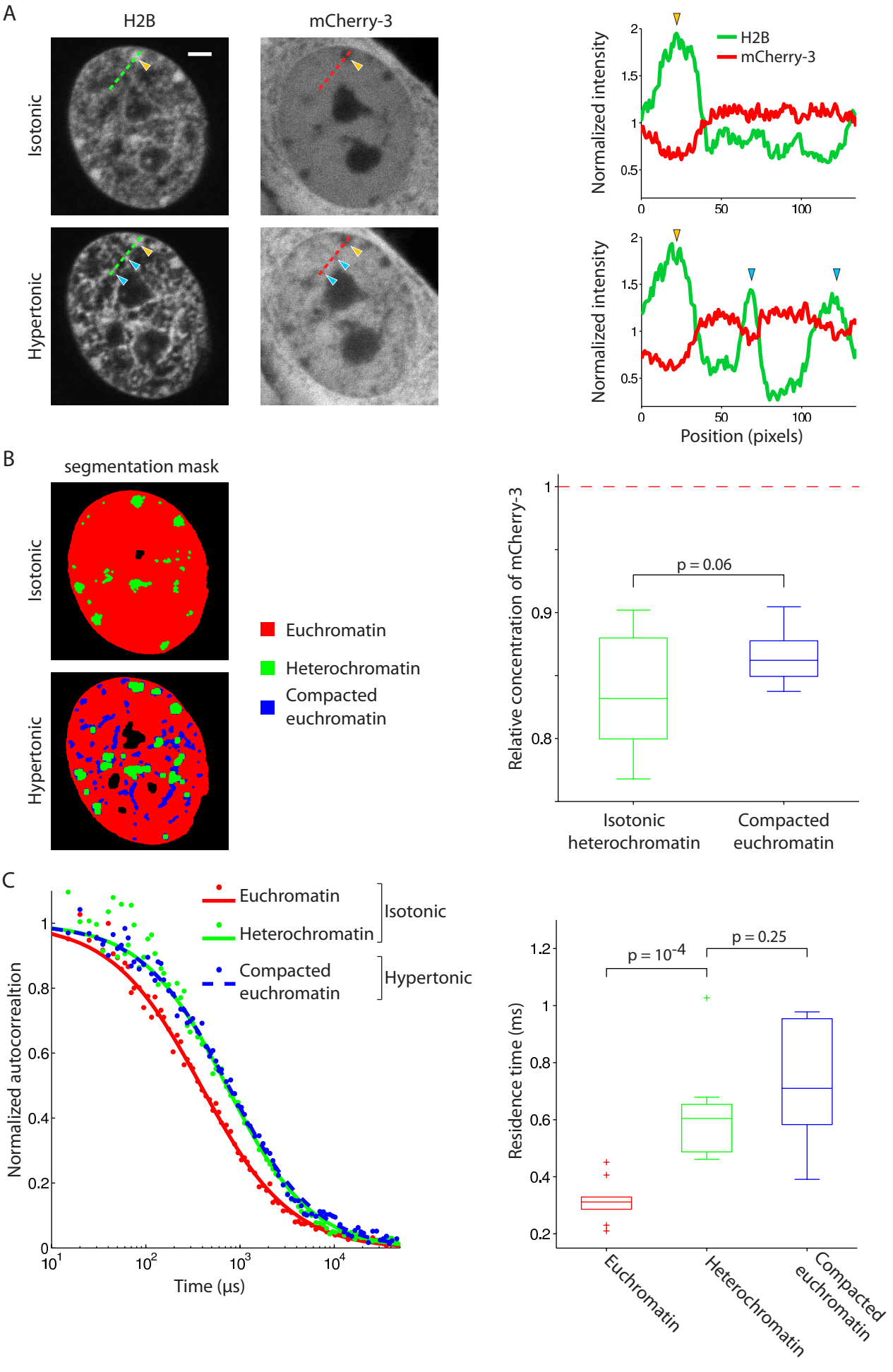

Walter et al., Figure 2

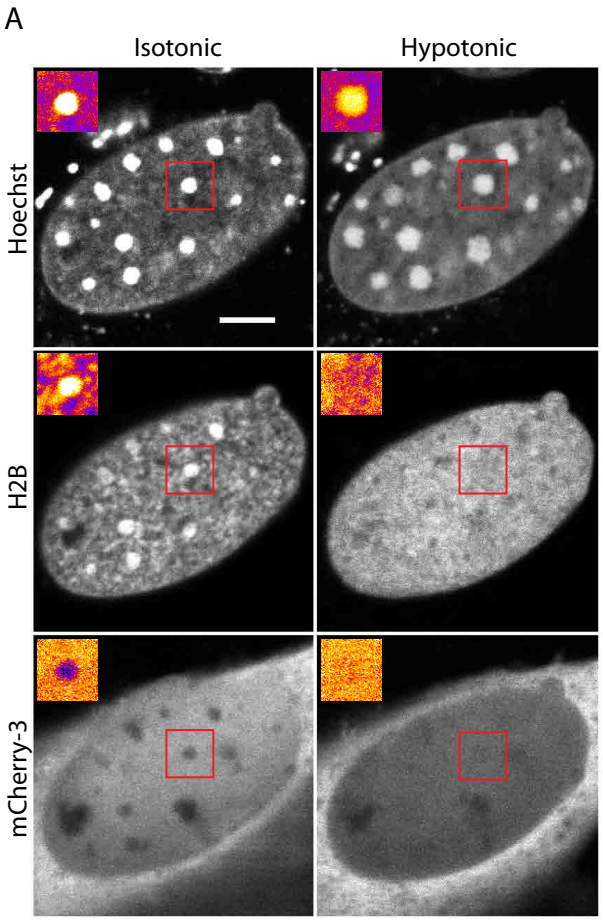

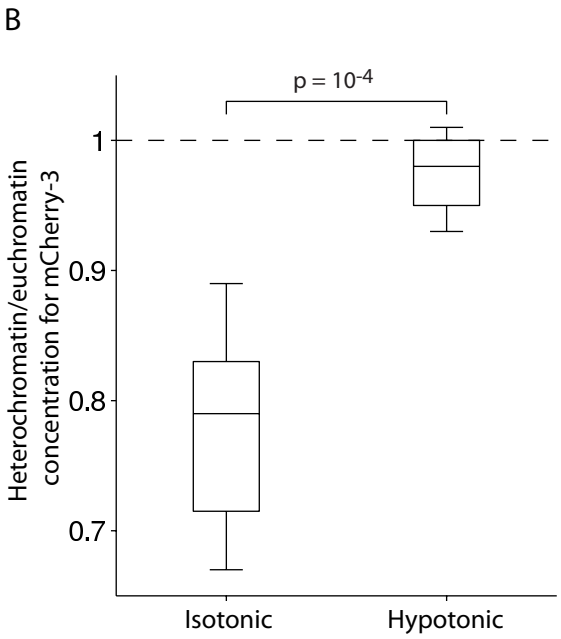

Walter et al., Figure 3

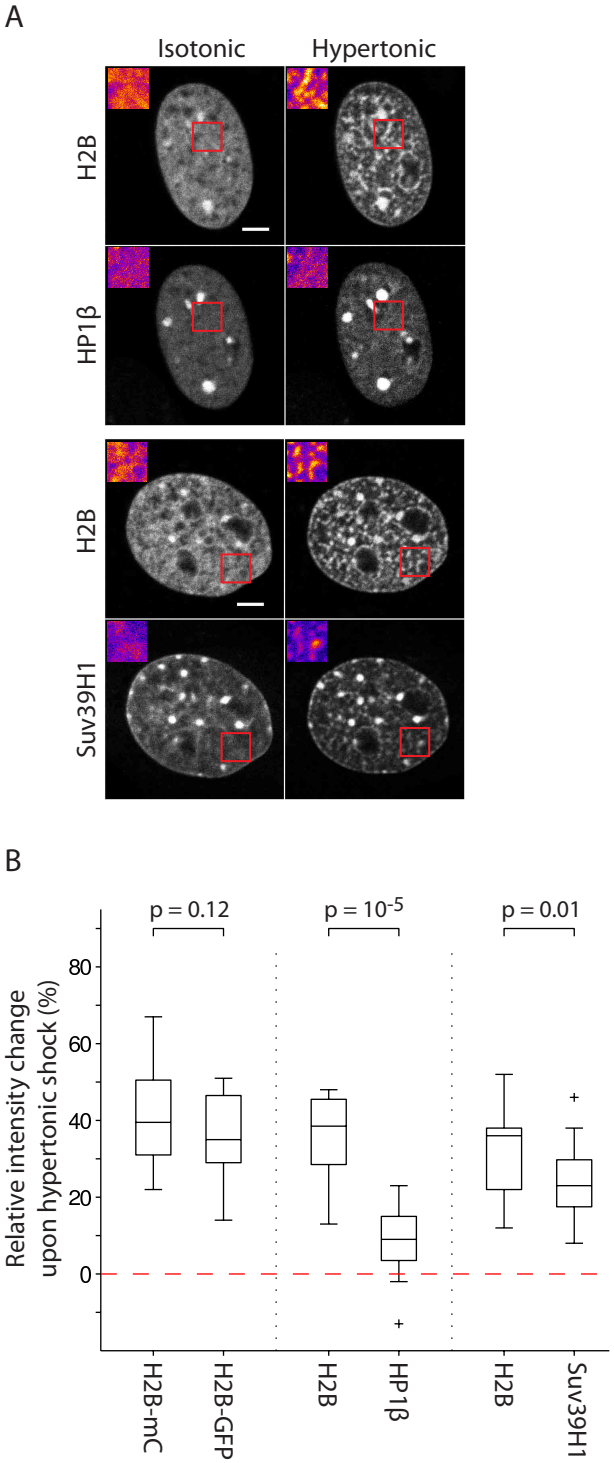

Walter et al., Figure 4

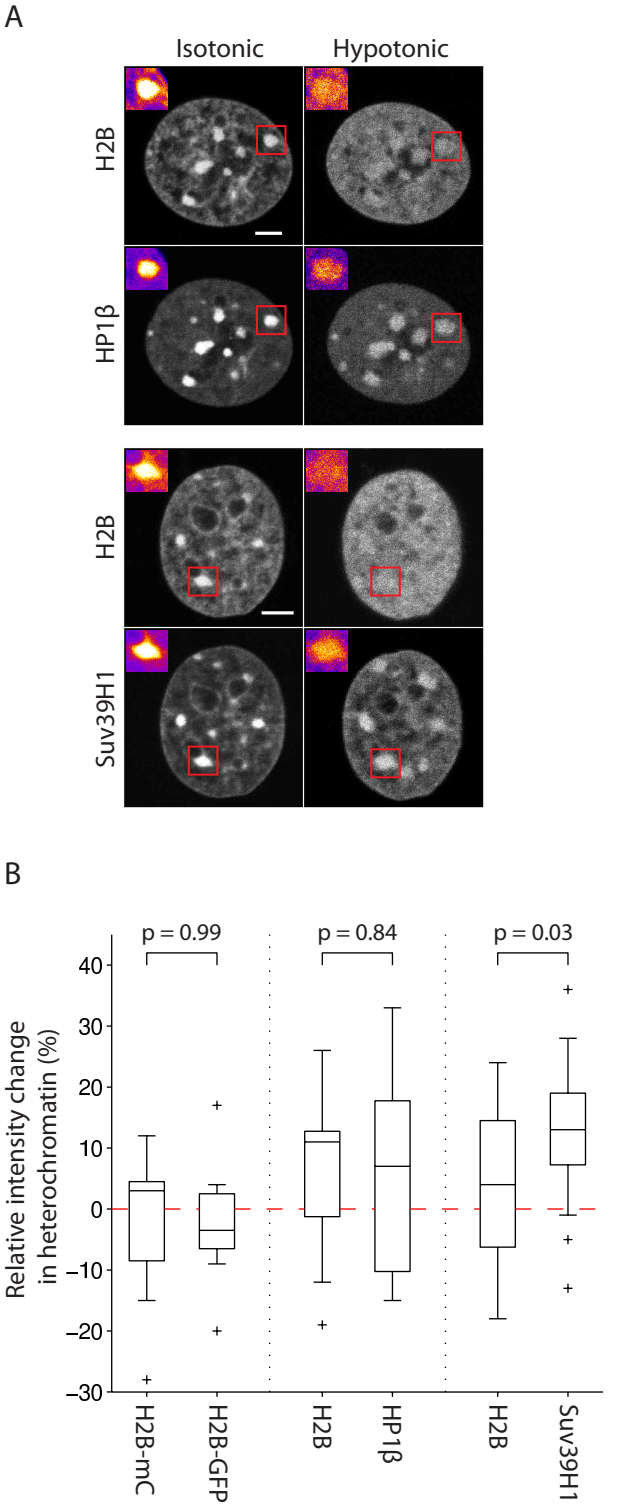
A
Isotonic
Hypotonic
H2B
HP1β
H2B
Suv39H1
B
p = 0.99
p = 0.84
p = 0.03
Relative intensity change in heterochromatin (%)
40
30
20
10
0
−10
−20
−30
H2B-mC
H2B-GFP
H2B
HP1β
H2B
Suv39H1
C
Isotonic
Hypotonic
15 min
45 min
3 h
H2B
H3K9me3